energies

MDPI

Article

Electrification of a Heavy-Duty CI Truck—Comparison of Electric Turbocharger and Crank Shaft Motor

Kristoffer Ekberg, Lars Eriksson * and Christofer Sundström

Division of Vehicular Systems, Department of Electrical Engineering, Linköping University, 581 83 Linköping, Sweden; kristoffer.ekberg@liu.se (K.E.); christofer.sundstrom@liu.se (C.S.)
* Correspondence: lars.eriksson@liu.se

Abstract: A combustion engine-driven vehicle can be made more fuel efficient over some drive cycles by, for example, introducing electric machines and solutions for electrical energy storage within the vehicle's driveline architecture. The possible benefits of different hybridization concepts depend on the architecture, i.e., the type of energy storage, and the placement and sizing of the different driveline components. This paper examines a diesel electric plug-in hybrid truck, where the powertrain includes a diesel engine supported with two electric motors, one supporting the crank shaft and one the turbocharger. Numerical optimal control was used to find energy-optimal control strategies during two different accelerations; the trade-off between using electrical energy and diesel fuel was evaluated using a simulation platform. Fixed-gear acceleration was performed to evaluate the contribution from the two electric motors in co-operation, and individual operation. A second acceleration test case from 8 to 80 km/h was performed to evaluate the resulting optimal control behavior when taking gear changes into account. A cost factor was used to relate the cost of diesel fuel to electrical energy. The selection of the cost factor relates to the allowed usage of electrical energy: a high cost factor results in a high amplification from electrical energy input to total system energy savings, whereas a low cost factor results in an increased usage of electrical energy for propulsion. The difference between fixed-gear and full acceleration is mainly the utilization of the electric crank shaft motor. For the mid-range of the cost factors examined, the crank shaft electric motor is used at the end of the fixed-gear acceleration, but the control sequence is not repeated for each gear during the full acceleration. The electric motor supporting the turbocharger is used for higher cost factors than the crank shaft motor, and the amplification from electrical energy input to total energy savings is also the highest.

Keywords: optimal control; hybrid electric vehicle; acceleration; electric motor; diesel engine

Citation: Ekberg, K.; Eriksson, L.; Sundström, C. Electrification of a Heavy-Duty CI Truck—Comparison of Electric Turbocharger and Crank Shaft Motor. *Energies* **2021**, *14*, 1402. https://doi.org/10.3390/en14051402

Received: 25 December 2020
Accepted: 23 February 2021
Published: 4 March 2021

1. Introduction

The commercial medium and heavy-duty fleet in Europe was at 2015 around 6 million trucks [1]. The challenge for the vehicle manufactures is now to develop new trucks with new fuel types, to deal with global warming and the European targets on vehicle emissions. In 2019 the majority of new registrations of medium and heavy trucks were for diesel vehicles (97.9%); 0.1% of the vehicles where hybrid electric vehicles (HEVs) [2]. The development of HEVs introduces new opportunities for the vehicle manufactures regarding how to control the vehicle, due to the extra energy source, in comparison to using only the internal combustion engine for propulsion. A HEV can be developed in many ways depending on the use of different energy sources, type and positioning of electric machines, power inverters, etc. An overview of the main components in an HEV is presented in [3]. In [4], six different HEV architectures are presented; the different architectures all combine a combustion engine with an electric machine, which are located at different positions in the driveline.

When a hybrid electric vehicle architecture is developed, the number of actuators is usually increased, since controllable components are added in the system. The task

of finding control strategies for the newly introduced electric components, together with the combustion engine, can be solved in different ways. In [5], a method for calculating control strategies for a given horizon based on the travel distance was calculated with the use of dynamic programming and Pontryagin's maximum principle. Another solution was proposed in [6]; a decentralized multi-layer control architecture was developed that decides on the power split between the electric motor and the combustion engine, the gear selections and the engine on/off state in three different layers, where, for example, the gear selection and engine on or off state are decided with dynamic programming. In [7], the fuel saving potential by hybridizing a class 8 line-haul truck was investigated, where a mild and a full hybrid with implemented control strategies were modeled and compared to a conventional truck model in a couple of different drive cycles. In [8], dynamic programming was used to find optimal control strategies for a hybrid electric vehicle, the optimal controls were implemented in a real-time lookup control strategy. Reference [9] compared two different problem formulations when solving a drive cycle problem with dynamic programming, where speed, or speed and distance, are states in the system model. Reference [10] used convex optimization techniques to scale the battery in an electric vehicle; they also used dynamic programming as a comparative case, but their convex method has faster calculation times than the dynamic programming solution.

Apart from supporting the engine main shaft with an electric motor, smaller electric motors could be included in the combustion engine architecture to assist the engine at some load points. Two types of strategies which increase the intake manifold pressure in the engine are having an electric compressor in series with the turbocharger compressor (as in [11]) and electric turbocharging [12,13]. The electrically assisted turbocharger has the possibility to improve the combustion engine acceleration time, as mentioned in [12] (p. 13): "substantial improvements can be achieved during the acceleration transients.". The turbo compounding technology results in the possibility to regenerate exhaust gas energy. The usage of such a system can reduce the fuel consumption for some use cases, by using either only the electric turbo [12], or by using both an E-crank system and an E-turbo [14].

The problem when introducing an electric turbocharger into the system is that the model needs to take the turbocharger dynamics into account; otherwise, some information about the turbocharger utilization might be lost. See, for example, Ref. [15], wherein a comparison is made between different optimal control methods and comparing an engine map model with an engine model taking the turbocharger dynamics into account.

In [16], time-optimal accelerations of a hybrid vehicle with a gasoline engine and an electric turbocharger were investigated by using dynamic programming and Pontryagin's maximum principle to find the optimal controls. Reference [16] also developed a model for taking the turbocharger dynamics into account, without explicitly modeling the states of the turbocharger's rotational speed or the intake manifold pressure.

In this paper, a parallel hybrid heavy-duty truck is modeled by extending an existing diesel engine model with two electric motors, a driveline model and a chassis model. The parallel hybrid configuration enables the possibility for the electric motor to assist the diesel engine during accelerations [17] (p. 62). The diesel engine model is a three-state mean value engine model, which takes the turbocharger dynamics into account. The turbocharger dynamics are important, since they have a large impact on the intake manifold pressure. The electric motor models are polynomial models developed in this paper, which correlate the input current and rotational speed with the delivered shaft power. One of the electric motors together with the combustion engine make the parallel hybrid system, while the second electric motor is used to electrically assist the turbocharger shaft. The electric boost system could have been modeled as either an electric compressor in series with the turbocharger (as in [11]), or as in, for example, Ref. [12–14], where the electric motor is placed on the turbocharger shaft. Since the solution when the electric motor is placed on the turbocharger shaft enables the possibility of generating electrical energy at some load points (as in, for example, Ref. [12]), this architecture was chosen for this investigation. The process of electrical energy generation is not examined in this work, but the possibility

of generating electrical energy, and the possible fuel savings, seems to favor the selected system architecture of having the electric motor on the turbocharger shaft.

To find the optimal control strategies which reduce the energy required to perform an acceleration, in terms of fuel and electrical energy, direct collocation is used. Constraints are implemented when solving the optimal control, to ensure that, for example, the engine air–fuel ratio limit and maximum torque of the electric machines are not violated. The optimal controls of the electric motors and their impacts on the diesel engine system during two different accelerations are analyzed. The benefits of having a parallel hybrid with an electrically assisted turbocharger during a short acceleration, and a full acceleration including gear changes, are analyzed for different cost ratios between diesel fuel and electrical energy.

1.1. Scenario

A model describing a 40,000 kg diesel powered truck, equipped with an electric motor on the crank shaft (E-crank) and an electric turbocharger (E-turbo), was used to find energy-optimal control strategies during accelerations. The aim was to perform an energy-optimal acceleration, while the engine speed was increased from 600 to 2000 rpm, using a fixed gear. The cost of the electric energy, in relation to diesel fuel, was adjusted to evaluate the system control strategies for the different relations of the cost using the two different energy sources. The control signals for the fuel injection, wastegate position and electric motor currents were calculated using numerical optimal control. The results show how the power should be divided between the two electric motors, depending on the ratio between fuel and electrical energy cost, and how the performance of the combined E-crank and E-turbo system differs from using either an E-crank or an E-turbo separately. Acceleration from 8 to 80 km/h was performed with both the E-crank and E-turbo active, to study the effects of the electric motors on a full acceleration using multiple gears.

1.2. Contributions and Research Question

This work contributes by developing a method for making comparisons between different electrification architectures, where the properties of the components are used at their full potential for the given task. The questions that the paper investigates and answers are:

- Is it beneficial to electrify both the main shaft and the turbocharger?
- When should the two electric motors be used, if the acceleration is to be more energy efficient than using only diesel fuel?
- Is it sufficient to study fixed-gear acceleration to find energy-optimal control strategies to apply during accelerations using multiple gears?

2. Vehicle Model

The system model in Figure 1 consists of sub-models for: combustion engine, driveline, chassis and electric motors. The hybrid configuration is a parallel hybrid, where the crank shaft electric motor is fixed to the engine crank shaft, and the electric turbocharger is fixed to the turbocharger shaft. The complete model consists of six states and six control signals. The states are the turbocharger rotational speed ω_{tc}, intake manifold pressure p_{im}, exhaust manifold pressure p_{em}, engine rotational speed ω_{ice}, wheel rotational speed ω_{wheel} and driven distance. The controls are fuel injection u_{fuel}, wastegate position u_{wg}, E-turbo current $i_{\text{em}}^{\text{tc}}$, E-crank current $i_{\text{em}}^{\text{crank}}$, clutch position u_{clutch} and gear selection u_{gear}. The selected gear is decided when setting up the problem, but the utilization time of each gear is a free variable. The energy source supplying electric power to the electric motors is assumed to be ideal. The states and controls in the model are described further in Section 2.4.

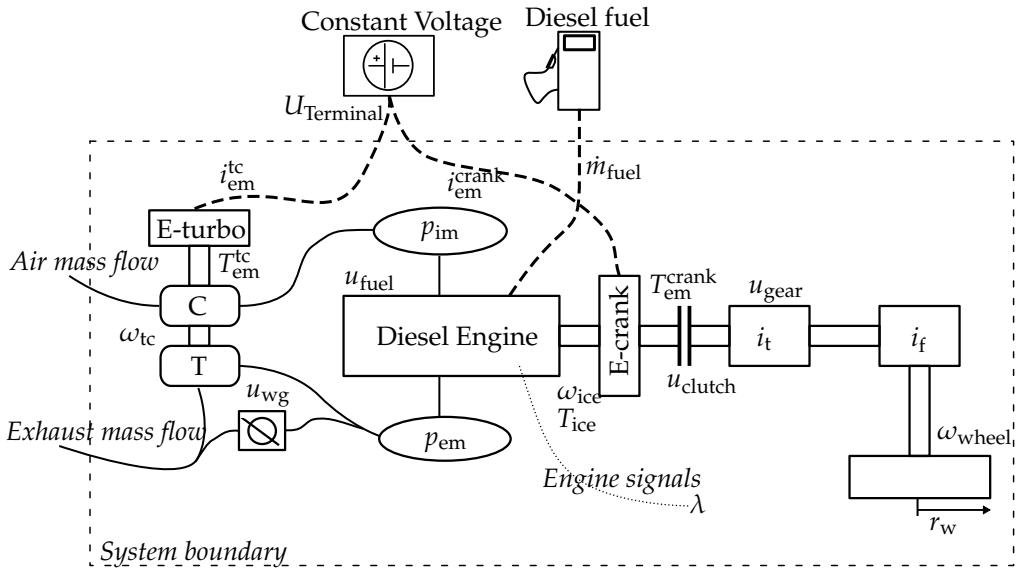

Figure 1. Terminology used to describe the diesel engine and the electric motors.

2.1. CI Engine Model

A previously developed and validated mean value engine model (MVEM) [18] is used to perform the acceleration. The model is further developed by introducing the electric motors in the system. The reference model contains a throttle between the compressor and the intake manifold volume p_{im}, but it is removed to reduce one state and one control signal. The model, as it is used, contains three modeled states: intake manifold pressure p_{im}, exhaust manifold pressure p_{em} and turbocharger rotational speed. The two controls are fuel injection u_{fuel} and wastegate position u_{wg}. The MVEM is suitable for optimal control of a vehicle's acceleration, since it captures the turbocharger and air path dynamics, which encapsulates the limiting dynamics of the diesel engine. In particular, the requirement on air–fuel ratio λ is especially important while performing accelerations. The engine full load air–fuel equivalence ratio is limited due to black exhaust smoke [19] (p. 656), which restricts the upper limit on the injected amount of fuel. The internal engine variables are implemented as constraints during the optimal control procedure. Examples of such variables are engine air–fuel ratio and the compressor surge limit. The compressor surge limit defines the maximum boost pressure for a given air mass flow. Surge limits the maximum boost pressure which can be achieved by the turbocharger compressor in the low speed engine region [20]. The engine stationary performance and the maximum torque limit is depicted in Figure 2. The torque restriction from 500 to 900 rpm is the stationary limit due to the air–fuel ratio $\lambda_{\text{limit}} = 1.3$. During the analysis, the air–fuel ratio limit is implemented, but the electric motor on the turbocharger is introduced, which can increase the intake manifold pressure and thereby the air mass flow to the cylinders. As a result, more fuel can be injected and the engine is capable of delivering more torque below 900 rpm than what is depicted in Figure 2. The boundaries on power and torque are still respected, the maximum power is set to 450 hp and the maximum torque to 2400 Nm.

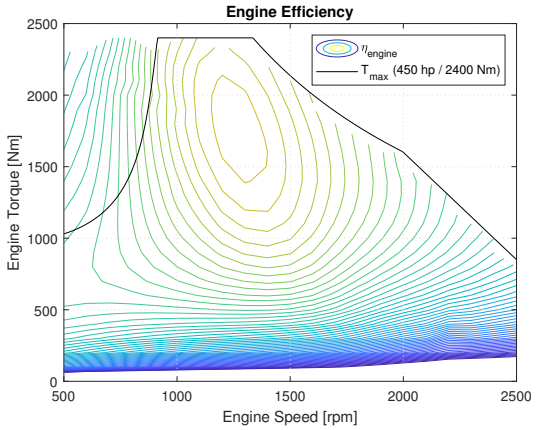

Figure 2. The stationary engine map for the MVEM. The maximum torque is set to 2400 Nm, the stationary air–fuel ratio limits the output torque to between 500 and 900 rpm, the maximum power is set to 450 hp and a high rpm cut-off is imposed at 2000 rpm. The diesel engine model's maximum efficiency is 46%.

2.2. Electric Motors

The electric motor model was developed with current and rotational speed as the input signals, and the shaft power as output. Measured data from a 59 kW permanent magnet synchronous motor included in an electric rear axle hybrid vehicle [21] were used as a reference when developing the electric motor model. The data contain the motor shaft power output, rotational speed, torque and the electric power input to the power inverter. The motor and power inverter are lumped together to one subsystem, and therefore direct current from the energy storage will be the input to the model. The system describing the electric motor and inverter is displayed in Figure 3, including the nomenclature, where the constant voltage source U_{terminal}, current i_{em}, the electric motor losses $k_{\text{loss}}(N_{\text{em}}, i_{\text{em}})$, shaft power P_{em} and shaft rotational speed N_{em} are displayed. The dashed line represents the system boundary.

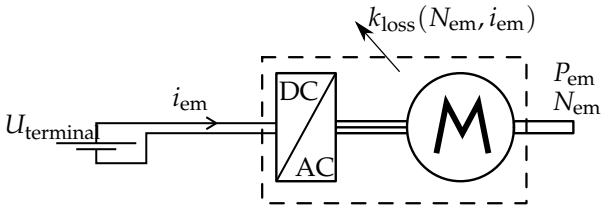

Figure 3. Terminology used to describe the electric motor. The dashed line represents the system's boundary. U_{terminal} is the voltage from a constant voltage power supply.

The estimated input current ($i_{\text{em}} = P_{\text{input}}/U_{\text{terminal}}$) and rotational speed were chosen as the input signal to the model and the shaft power as output signal. P_{input} is the electric power input to the inverter. Data were only available for one electric motor and inverter system; therefore, the resulting model was scaled according to the power conservation with an ideal gear ratio, to ensure that the motor performance matches the speed ranges of either the E-crank or the E-turbo applications. Using such a gear ratio would not be suitable in a real world application, since a high-speed motor would probably be needed for the turbocharger. The scaling was only used to develop working maps for the two different electric machines. Electric machines of suitable speed ranges can be developed; see, for example, Ref. [22], where a prototype electric machine was developed for an electric turbocharger application. The power limits for the two motors were adjusted to match the application. A general electric motor model was developed, where the considered losses

are shaft friction, iron losses and copper losses due to the current. The power losses in the electric motor model are described with the function:

$$k_{\text{loss}}(N_{\text{em}}, i_{\text{em}}) = c_0 + c_1 N_{\text{em}} + c_2 N_{\text{em}}^2 + c_3 i_{\text{em}}^2 + c_4 \frac{i_{\text{em}} U_{\text{terminal}}}{N_{\text{em}}} \quad (1)$$

where N_{em} is the rotational speed, c_0 describes the iron losses, c_1 and c_2 are the linear and quadratic gain parameters describing the friction, c_3 is the motor resistance and i_{em} is the electric current into the inverter. The component $c_4 \frac{i_{\text{em}} U_{\text{terminal}}}{N_{\text{em}}}$ is included to reduce the motor efficiency at high torque. The motor current and input voltage do not represent the shaft torque directly, due to the power losses in the electric motor, but seem to work in order to give the model more freedom in shaping the resulting efficiency map. The electric motor power, efficiency and torque are calculated as:

$$P_{\text{shaft}} = U_{\text{terminal}} i_{\text{em}} - k_{\text{loss}}(N_{\text{em}}, i_{\text{em}}) \quad (2)$$

$$\eta_{\text{em}} = \frac{P_{\text{shaft}}}{U_{\text{terminal}} i_{\text{em}}} \quad (3)$$

$$T_{\text{em}} = \frac{P_{\text{shaft}}}{N_{\text{em}} \frac{\pi}{30}} \quad (4)$$

where P_{shaft} is the shaft power, η_{em} is the electric motor efficiency, T_{em} is the shaft torque and U_{terminal} is the terminal voltage. The terminal voltage is assumed to be supplied from an ideal constant voltage energy storage onboard the vehicle.

2.2.1. Electric Motor Model Validation

The model is fitted to data by minimizing the difference in measured shaft power and the modeled shaft power (2). During the model parametrization, the parameters are lower bounded to zero since the parameters describe the losses in the electric motor. In Table 1, the statistics R^2 of the model fit, error residual mean value and standard deviation are displayed. The confidence intervals of the mean value and standard deviation from fitting a normal distribution (using *fitdist* function in the MATLAB toolbox [23]) to the error residual are also shown. The R^2 value indicates how well the variations in the data are captured by the model. A mean value near zero and a low standard deviation indicate a model with good fit. The power output validation in the left plot in Figure 4 shows that the model and the data seem to describe a similar power output behavior. The efficiency plot in Figure 4, show that the model captures the efficiency island levels. Even though the efficiency model fit is not perfect, the model is considered to be good enough to be used in the optimal control problem. The right plot in Figure 4 shows the relation between the modeled shaft power and the measured shaft power. The model underestimates some of the low power points, but apart from that, the model seems to represent the main features in the data.

Table 1. Statistics from the electric motor model parametrization.

Statistic	Value	Confidence Interval
R^2 [-]	0.99918	
Mean value of error residual [W]	−24.2	−73.6, 25.2
Standard deviation of error residual [W]	468.4	436.0, 506.1

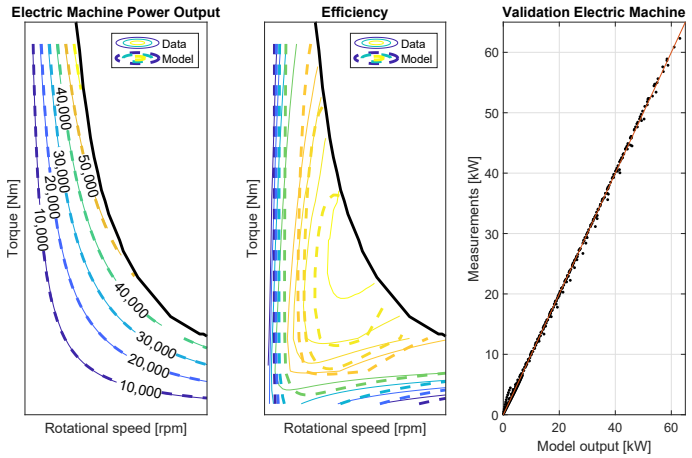

Figure 4. Electric motor power output and efficiency, and a comparison of the model's power output and the measured power output. Note that the highest efficiency island is not captured by the model.

2.2.2. Electric Motor Scaling for E-Turbo and E-Crank

The electric motor models used on the engine crank shaft and turbocharger shaft have different maximum power, maximum speed speed and maximum torque demands. Since only data from one motor map were available, the motor model was scaled with a gear ratio to convert the rotational speed and torque to represent the motors with different requirements. There are three measures which are considered when scaling the electric motor model. Those are maximum torque, maximum rotational speed and maximum power. The required torque, rotational speed and power output for the two electric motors are displayed in Table 2. The crank shaft motor is sized for a continuous power of 75 kW and a maximum torque of 870 Nm. The electric turbocharger motor is sized for a continuous power of 25 kW and a maximum torque of 6 Nm.

The resulting efficiency maps for the E-crank and E-turbo motors are depicted in Figures 5a,b. The relation between maximum torque and rotational speed in the original map is kept when scaling the two new motors. The maximum output power for the crank shaft motor is limited to 75 kW and the turbocharger motor is limited to 25 kW.

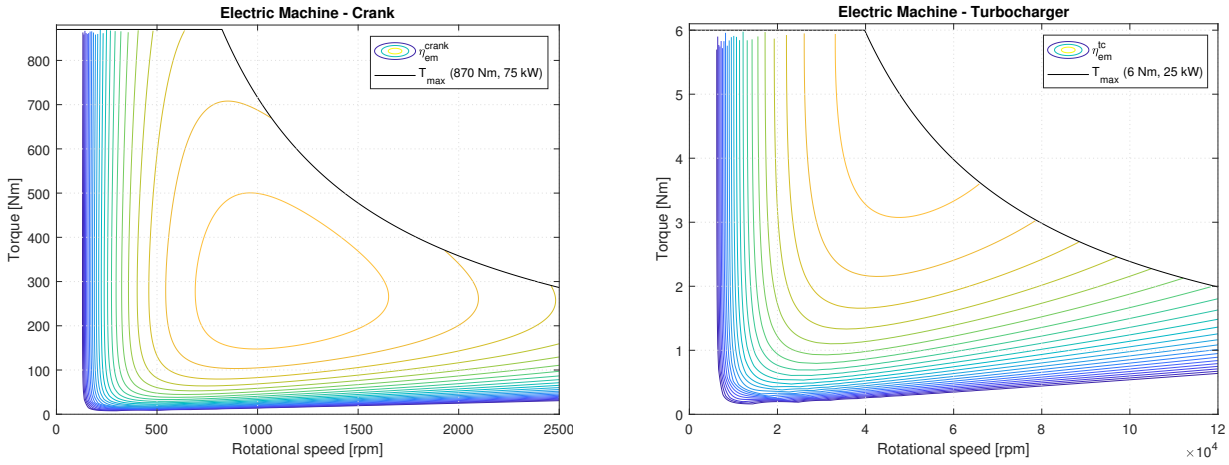

(**a**) (**b**)

Figure 5. Electric motor characteristics for (**a**) crank shaft motor efficiency lines and the maximum torque restriction, and (**b**) turbocharger efficiency lines and the maximum torque restriction. The maximum efficiency reached by the combined electric motor and inverter for the two models was 92%.

Table 2. Electric motor model's requirements.

Motor	Turbocharger	Crank
Maximum power [kW]	25	75
Maximum torque [Nm]	6	870
Maximum rotational speed [rpm]	120,000	2500

2.3. Chassis

The chassis model, gearbox and final drive ratios are from [24]. The driveline model is considered to be stiff. The 6th gear is used during the short acceleration missions. The truck during this mission was a semi-trailer, with a weight of 40,000 kg. Due to the weight of the truck, and the semi-trailer configuration, there was no risk of wheel slip when starting with the 6th gear at slow rolling speed. Performing the calculations to find out how much torque the engine can deliver before the wheels slip on dry tarmac resulted in a maximum engine torque of 6.4 kNm. The calculations were performed according to Equation (3.19) in [25] (p. 221), using the vehicle parameters from [25] (p. 304). Since the maximum torque of the engine model was set to 2400 Nm, and the E-crank to 870 Nm, there was no risk of wheel slip during the mission, and a rolling condition was therefore assumed to connect the vehicle speed to the wheel rotational speed.

2.4. State Descriptions

There are six states and six control signals in the complete model (depicted in Figure 1). The model states are: wheel rotational speed ω_{wheel}, engine rotational speed ω_{ice}, intake manifold pressure p_{im}, exhaust manifold pressure p_{em}, turbocharger rotational speed ω_{tc} and driven distance d_{vehicle}. The engine control signals are: fuel injection u_{fuel}, wastegate position u_{wg}, E-turbo current $i_{\text{em}}^{\text{tc}}$ and E-crank current $i_{\text{em}}^{\text{crank}}$. Besides these, the clutch and gear are also controlled. When solving the full acceleration mission, the clutch control signal is used to synchronize the rotational speeds of the engine and the upcoming gear, and the gear is decided when setting up the optimal control problem. More information about the full acceleration model will follow in Section 3.2.3. The reader is referred to [18] for more detailed descriptions about the engine states and model equations. The states are summarized as:

$$\dot{\omega}_{\text{wheel}} = \frac{\dot{\omega}_{\text{ice}}}{i_{\text{f}} i_{\text{t}}} \tag{5}$$

$$\dot{\omega}_{\text{ice}} = \frac{1}{J_{\text{vehicle}}} \left(T_{\text{ice}}(u_{\text{fuel}}, u_{\text{wg}}) + T_{\text{em}}^{\text{crank}}(i_{\text{em}}^{\text{crank}}, \omega_{\text{ice}}) - T_{\text{wheel}}(\omega_{\text{wheel}}) / i_{\text{f}} i_{\text{t}} \right) \tag{6}$$

$$\dot{p}_{\text{im}} = \ldots \tag{7}$$

(The state description can be found in [18])

$$\dot{p}_{\text{em}} = \ldots \tag{8}$$

(The state description can be found in [18])

$$\dot{\omega}_{\text{tc}} = \frac{1}{\omega_{\text{tc}}(J_{\text{tc}} + J_{\text{em}}^{\text{tc}})} \left(P_{\text{t}} \eta_{\text{tm}} - P_{\text{c}} + \omega_{\text{tc}}\, T_{\text{em}}^{\text{tc}}(i_{\text{em}}^{\text{tc}}, \omega_{\text{tc}}) \right) \tag{9}$$

$$\dot{d}_{\text{vehicle}} = \omega_{\text{wheel}}\, r_{\text{wheel}} \tag{10}$$

where J_{vehicle} collects the driveline inertias, and is described as:

$$J_{\text{vehicle}} = J_{\text{ice}} + J_{\text{em}}^{\text{crank}} + J_{\text{t}} + \frac{J_{\text{f}} + J_{\text{wheel}} + m_{\text{vehicle}} r_{\text{wheel}}^2}{i_t^2 i_f^2} \tag{11}$$

which collects the rotating component inertias for the: engine J_{ice}, gearbox J_{t}, final drive J_{f}, wheel J_{wheel} and the equivalent rotating inertia associated with the vehicle mass $m_{\text{vehicle}} r_{\text{wheel}}^2$ due to the rolling condition. The electric power consumed from the power supply is described as:

$$\dot{E}_{\text{supply}} = P_{\text{em}}^{\text{turbo}} + P_{\text{em}}^{\text{crank}} = U_{\text{terminal}}(i_{\text{em}}^{\text{crank}} + i_{\text{em}}^{\text{tc}}) \tag{12}$$

where U_{terminal} is the constant voltage source, $i_{\text{em}}^{\text{crank}}$and $i_{\text{em}}^{\text{tc}}$ are the currents of the electric motors. The vehicle is assumed to have a stiff driveline; therefore, the wheel speed is strictly decided from the engine speed, via the gearbox with gear ratio i_{t} (which also depend on the selected gear u_{gear}) and final drive with gear ratio i_{f}. The electric motors produce the torques $T_{\text{em}}^{\text{crank}}$ and $T_{\text{em}}^{\text{tc}}$, which are acting on the engine crank shaft and the turbocharger shaft. The engine and turbocharger rotational speeds are decided using newtons second law. The torque balance together with the system inertias decide the angular acceleration for each state. The system inertias are engine inertia J_{ice}, turbocharger inertia J_{tc}, E-turbo inertia $J_{\text{em}}^{\text{tc}}$, E-crank inertia and $J_{\text{em}}^{\text{crank}}$. The torque needed on the wheels to propel the vehicle $T_{\text{wheel}}(\omega_{\text{wheel}})$ is calculated as in [24], while assuming flat road. The wheel rotational speed ω_{wheel} is multiplied with the radius of the wheel r_{wheel} to receive the vehicle speed, which is used to calculate the aerodynamic and rolling resistance forces acting on the vehicle.

3. Problem Formulation

The problem is to accelerate the truck to a target engine speed $N_{\text{engine}}^{\text{final}}$, from a specified initial condition $x_{\text{initial state}}$. The cost which is minimized during the acceleration is the integral over time of the fuel power ($Q_{\text{LHV}}^{\text{Diesel}}\, \dot{m}_{\text{fuel}}$) and electrical power ($\dot{E}_{\text{supply}}$). During the acceleration the vehicle will cover some distance, so in order to take the driven distance into account, a reference case is specified. The reference case is a fuel optimal acceleration, where $i_{\text{em}}^{\text{crank}}$and $i_{\text{em}}^{\text{tc}}$are restricted to zero, with equal initial and final conditions as the solutions using electrical energy. The distance covered by the reference solution $d_{\text{vehicle}}^{\min \dot{m}_{\text{fuel}}}$ is used as a lower boundary on driven distance for all the solution when electrical energy is allowed. By specifying the requirement of distance covered, the useful work from each mission is guaranteed. If the distance requirement is not kept, there is a risk of having faster accelerations using electrical energy, which will result in worse mean fuel consumption (consumed fuel mass per driven meter) while not fulfilling the same transportation mission as the minimum fuel solution.

To perform an energy-optimal acceleration, the following problem is formulated:

$$\min_{u} \quad \int_{t_0}^{t_{\text{f}}} Q_{\text{LHV}}^{\text{Diesel}}\, \dot{m}_{\text{fuel}} + \beta \dot{E}_{\text{supply}}\, dt \tag{13}$$

$$s.t. \quad \dot{x} = f(x,u) \tag{14}$$

$$x_{\min} \leq x \leq x_{\max} \tag{15}$$

$$u_{\min} \leq u \leq u_{\max} \tag{16}$$

$$h(x,u) \leq 0 \tag{17}$$

$$x(t_0) = x_{\text{initial state}} \tag{18}$$

$$u(t_0) = u_{\text{initial control}} \tag{19}$$

$$N_{\text{engine}}(t_{\text{f}}) = \omega_{\text{ice}}(t_{\text{f}}) \frac{60}{2\pi} = N_{\text{engine}}^{\text{final}} \tag{20}$$

$$d_{\text{vehicle}}(t_{\text{f}}) \geq d_{\text{vehicle}}^{\min \dot{m}_{\text{fuel}}} \tag{21}$$

where the total energy input to the system is minimized (13), while the state dynamics (14) are fulfilled. The end time of the optimal control problem t_{f} is a free variable. The states (15) and controls (16) shall be kept within their specified boundaries. The maximum torque and power restrictions for the electric motors and combustion engine, and restrictions of

internal variables in the combustion engine, such as the air–fuel ratio, maximum engine torque and compressor surge, are implemented in (17). The problem initial conditions are strictly defined by the initial states (18) and initial controls (19). At the final time t_f there are three criteria: the engine rotational speed should be equal to $N_{\text{engine}}^{\text{final}}$ (20); the driven distance should be at least the distance covered by the solution when neither the E-turbo nor E-crank was allowed (21); and the engine states should be stationary. The most important constraints in (17) can be written as:

$$\lambda_{\text{limit}} \leq \lambda = \frac{\dot{m}_{\text{air}}}{AF_s\, \dot{m}_{\text{fuel}}} \tag{22}$$

$$P_{\text{ice}}^{\text{max}} \geq T_{\text{ice}}(u_{\text{fuel}}, u_{\text{wg}})\, \omega_{\text{ice}} \tag{23}$$

$$T_{\text{ice}}^{\text{max}} \geq T_{\text{ice}}(u_{\text{fuel}}, u_{\text{wg}}) \tag{24}$$

$$P_{\text{limit}}^{\text{crank}} \geq P_{\text{em}}^{\text{crank}} \tag{25}$$

$$T_{\text{limit}}^{\text{crank}} \geq T_{\text{em}}^{\text{crank}}(i_{\text{em}}^{\text{crank}}, \omega_{\text{ice}}) \tag{26}$$

$$P_{\text{limit}}^{\text{tc}} \geq P_{\text{em}}^{\text{tc}} \tag{27}$$

$$T_{\text{limit}}^{\text{tc}} \geq T_{\text{em}}^{\text{tc}}(i_{\text{em}}^{\text{tc}}, \omega_{\text{tc}}) \tag{28}$$

$$\Pi_{\text{surge}}^{\text{limit}}(\omega_{\text{tc}}) \geq \Pi_{\text{comp}} = \frac{p_{\text{im}}}{p_{\text{ambient}}} \tag{29}$$

where λ is described by the stoichiometry ratio AF_s, air mass flow $\dot{m}_{\text{air}}$ and fuel mass flow $\dot{m}_{\text{fuel}}$ into the cylinders. The compressor surge limit $\Pi_{\text{surge}}^{\text{limit}}$ depends on the turbocharger rotational speed ω_{tc}. The compressor pressure ratio Π_{comp} is defined as the intake manifold pressure p_{im} divided by the pressure before the compressor, which in this case is assumed to be ambient pressure p_{ambient} (see Figure 1).

3.1. Choice of Lagrange Function

One important aspect of using optimal control is to solve the "right" problem. Depending on the chosen Lagrange function (13), different solutions for the optimal control problem will be attained. Minimizing time instead of fuel would probably result in a solution where the combustion engine runs on full power during the whole transient. The chosen Lagrange formulation reduces the need of having $\dot{E}_{\text{supply}}$ as a state in the model; it is only needed in the cost function since there are no constraints on the amount of consumed electrical energy. The consumed electrical energy is calculated after the problem is solved. A selected range of β values is used to compare different relations in cost of electrical energy in comparison to using diesel. For example, $\beta = 1$ results in an equal cost per Joule of using diesel fuel and electrical energy.

3.2. Solving the Optimal Control Problem

To solve the energy-optimal acceleration described in (13)–(21), direct collocation is used to discretize the optimal control problem into a nonlinear program (NLP). The optimal control problem is formulated in MATLAB (R2019b) using YOP [26], which in turn uses the symbolic framework CasADi [27] to formulate the NLP. The NLP is solved using IPOPT [28], running with linear solver MUMPS.

3.2.1. Initial Guess

An initial guess for the acceleration mission is constructed by simulating the system dynamics, starting at the specified initial point. During the simulation the control signals are kept constant, and the current to the electric motors are set to zero. For the full acceleration mission, the initial guess is also simulated with constant control signals for each gear, except from the clutch control signal, which is assumed to have a constant closing speed.

3.2.2. Calculating the Optimal Control

The calculations were performed on an Intel(R) Core(TM) i7-8550U laptop with a 2.0 GHz quad-core processor and 16 GB of RAM. Using 100 control intervals during the fixed-gear mission results in an average calculation time of 76 s for each solution, when running five solvers in parallel, solving the fixed-gear acceleration. When solving the 8–80 km/h acceleration the mean calculation for the four solutions is around 9 min. The discretization of the problem for the full acceleration is 100 control intervals per in gear phase—five during the speed synchronization phase and 10 during the clutch closing phase. The calculation time is too long to be useful in a real time implementation, but the results give valuable insights in the trade-off between the different hybridization strategies.

3.2.3. Acceleration to 80 km/h with Gear Changes

To set up the mission of accelerating the truck to 80 km/h, and changing gears, the method in [29] was used, and the updated model for the clutch torque used in [30] was implemented. The criterion for when a gear change can be made (the end of the in gear phase) was set to:

$$c_{\text{gear change}}(t_{\text{f}}^{\text{in gear}}) = T_{\text{em}}^{\text{crank}} + T_{\text{ice}} = 0; \tag{30}$$

the shaft torque from the engine T_{ice} and E-crank $T_{\text{em}}^{\text{crank}}$ should sum to zero in the final time step of each in gear phase $t_{\text{f}}^{\text{in gear}}$. The Lagrange function in (13) is applied as the the cost function in all phases of the problem. The E-crank is not allowed to deliver any torque during the synchronization or clutch closing phase, to reduce unnecessary clutch wear. The end requirements in the final phase are that the vehicle speed should be at least 80 km/h, the engine states should be stationary and the driven distance should be at least the same as the distance covered by the minimum fuel solution.

4. Results—Fixed Gear Acceleration

The results from the three combinations of allowing electrical support while performing a fixed-gear acceleration are displayed in Figure 6. The solutions for a selected set of β-values are displayed. The results in Figure 6 show that the combination of using both the E-turbo and the E-crank motor results in the largest fuel consumption reduction, compared to using either the E-crank or E-turbo motor separately. When allowing the engine to deliver more torque than the stationary fuel limit, the torque delivery from the engine is the highest when the engine speed is around 800 rpm; if the E-turbo is used, see Figure 7a. The system is implemented as displayed in Figure 1, which means that the electric motors are always connected to the engine and turbocharger shafts. When the current to the electric motors is low, the friction in the motors puts some load on the shafts.

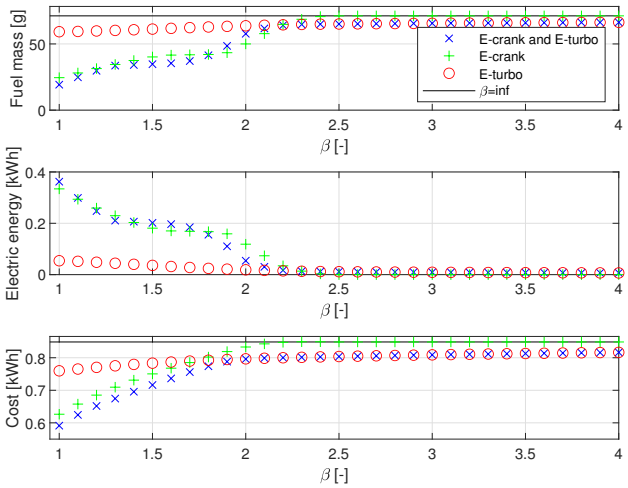

Figure 6. Cost factor β in relation to fuel mass consumed (**top**), electrical energy (**middle**) and optimal control cost (**bottom**). An increasing β corresponds to higher cost of electrical energy. β = inf is the resulting consumed fuel mass if an acceleration is performed without electrical assistance. The cost in the bottom figure is described in (13).

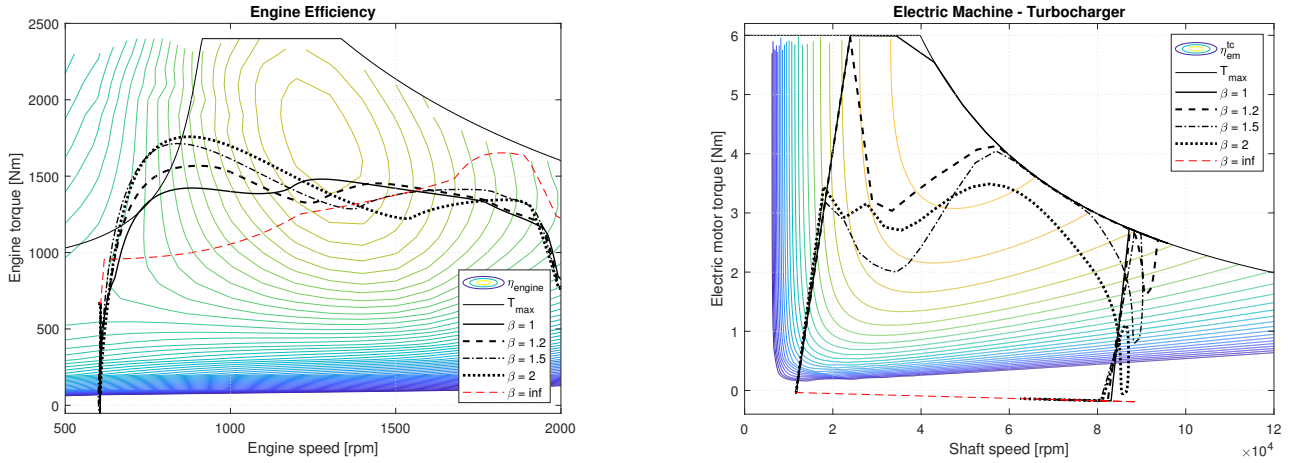

(**a**) (**b**)

Figure 7. Solution characteristics when using a combustion engine and a turbocharged electric motor. The legends display the cost factors (β) for the different solutions. (**a**) Diesel engine utilization during an energy-optimal acceleration with E-turbo. (**b**) Utilization of the E-turbo during the acceleration. When β = inf, the electric motor torque is negative due to friction.

4.1. Pareto Analysis—E-Crank

The green + in Figure 6 shows the consumed fuel mass in relation to the cost factor β, when only the E-crank is active. When $\beta < 2.5$ electrical energy is usage to propel the vehicle. If the electrical energy is more than 2.5 times the cost of diesel fuel ($\beta > 2.5$), the acceleration is performed on mainly diesel fuel.

4.2. Pareto Analysis—E-Turbo

The red ∘ in Figure 6 shows the results from using only the E-turbo as support to the diesel engine. Using the E-turbo results in a reduction of the consumed fuel mass for both low and high costs of the electrical energy. Both the consumed amount of electrical energy and possible fuel reduction are less than for the E-crank. However, there is a possibility of reducing the consumed fuel mass even when the cost of using electrical energy is high.

4.3. Pareto Analysis—E-Crank and E-Turbo

The blue × in Figure 6 shows the results from using both the E-turbo and E-crank. The benefits from the two different electric concepts add up. Using both electric motors adds the benefits from the fuel saving at lower values of β when using the E-crank, while also benefiting from the fuel consumption reduction from the E-turbo when the electrical energy gets more expensive.

4.4. Trajectory Analysis—E-Turbo

The electrical energy spent on spinning up the turbocharger increase the boost pressure (p_{im} in Figure 8), which unlocks the possibility to inject more diesel in the engine without being smoke limited, and consequently output more torque. In Figures 7a,b the results for five selected solutions with different values of β are displayed. When using only diesel, β = inf, the engine is smoke limited between 600 and 1300 rpm. When the usage of electrical energy is introduced, the extra supplied air enables a higher torque output at lower engine rpm's, this is visible in Figure 8, in the lower left plot displaying $1/\lambda$, when comparing β = inf solution with the other solutions where electrical energy is used. When β = 1 the E-turbo runs on full power, while the engine torque is around 1400 Nm during the acceleration. Figure 8 show the fuel-air ratio, intake manifold pressure, and the four control signals. The current to the turbocharger $i_{\text{em}}^{\text{tc}}$ show that the E-turbo is continuously used when β is low. When β increase, the E-turbo current is reduced in the middle of the transient while the fuel injection is increased during the first four seconds. The current to

the E-turbo is reduced in the middle of the diesel engine speed range, where the diesel engine efficiency is high and runs on excess air. The wastegate u_{wg} is open in the very beginning for all solutions, this can be seen in Figure 8. When the injected amount of fuel is increased, the wastegate is closed to convert the exhaust energy to useful work at the compressor. Figure 8, show an increasing intake manifold pressure p_{im}, for reduced values of β.

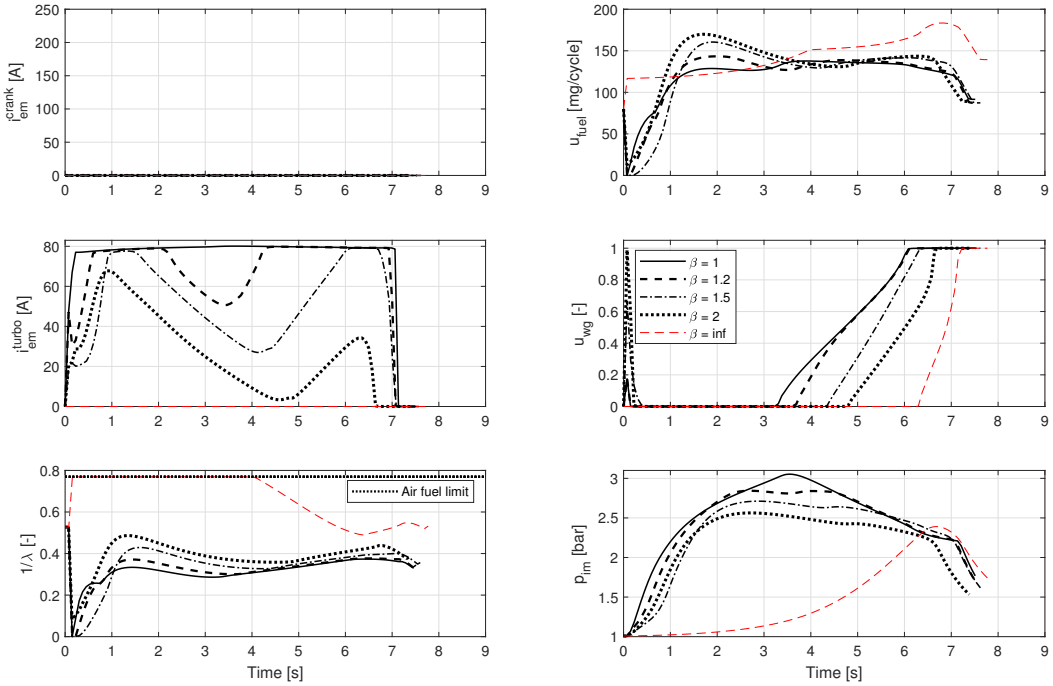

Figure 8. Controls, fuel-air ratio and intake manifold pressure, when the E-turbo is used to support the engine during the acceleration.

4.5. Trajectory Analysis—E-Crank

The load points in the crank shaft motor map, displayed in Figure 9b, show an increased usage with decreased cost on electrical energy. When β is large, the crank shaft motor is used in the beginning and in the end of the acceleration. The stationary engine map and a set of solutions are displayed in Figure 9a, which show that the engine torque is reduced, and the torque from the electric motor is increased, when β is lowered. An increased usage of the E-crank directly reduce the injected amount of fuel. This can be seen in Figure 10, where the fuel injection is reduced for the solutions where β is small. When β = 1.5, the E-crank runs on full power, while the diesel engine torque gradually increases as the engine rotational speed increase. The figure also shows that the diesel engine is limited by the air–fuel ratio in the beginning of the acceleration, until the support from the E-crank is enough for the diesel engine to reduce the fuel injection.

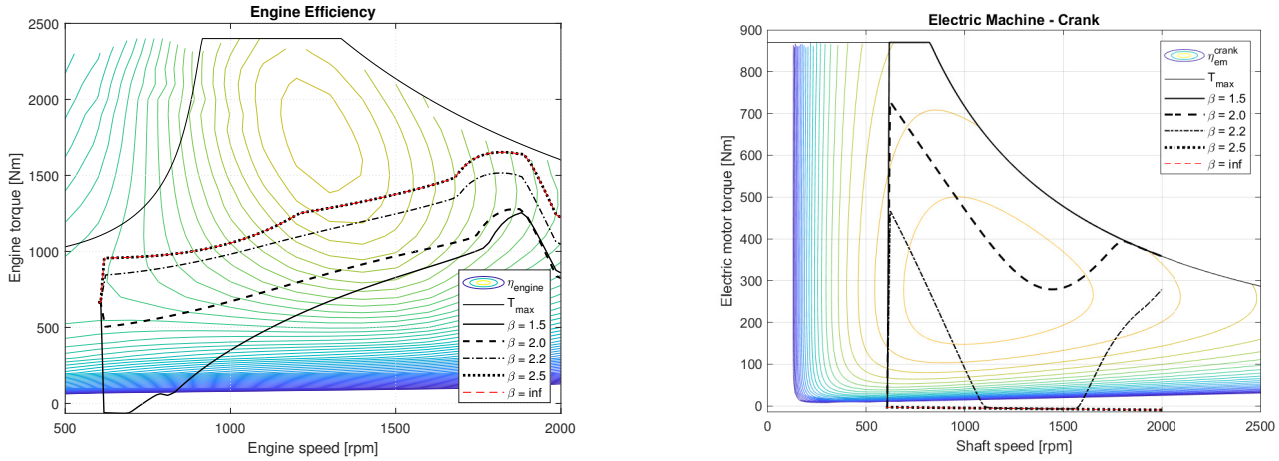

Figure 9. Solution characteristics when using a combustion engine and a crank shaft electric motor. The legends display the cost factors (β) for the different solutions. (**a**) Diesel engine utilization during a fuel optimal acceleration with E-crank. (**b**) Utilization of the E-crank during the acceleration. When β = inf, the electric motor torque is negative due to friction.

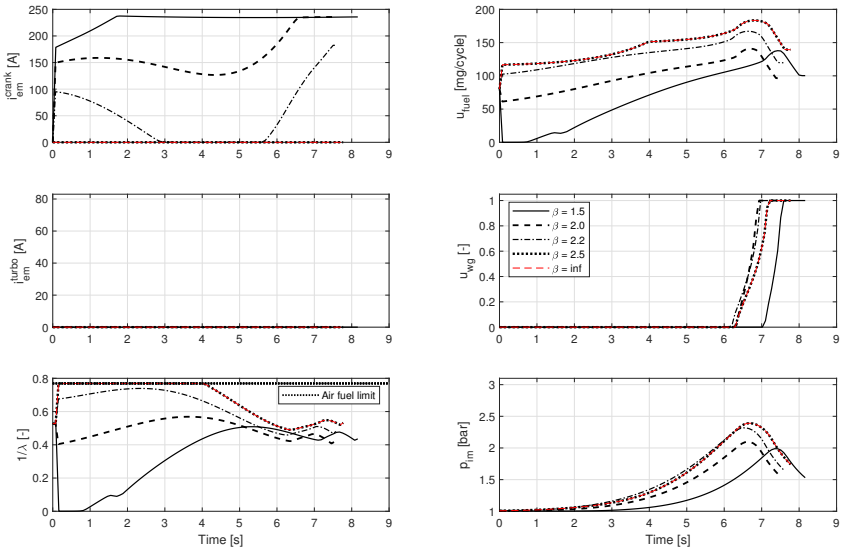

Figure 10. Controls, fuel-air ratio and intake manifold pressure during the acceleration when the E-crank is used to support the engine.

4.6. Trajectory Analysis—E-crank and E-turbo

Using both E-crank and E-turbo, the benefits from both the electric motors are available. The results in Figure 11a–c show that when β = 1.6, the diesel engine is not used until the engine speed exceed 1000 rpm. When β increases, the diesel engine is used together with the two electric motors. Concentrating on β = 1.6, 2.0 and 2.1 in Figure 12, show that the E-crank is used for propulsion, while the E-turbo current is high at the beginning of each gear. The more expensive the electrical energy becomes, the earlier the combustion engine starts to inject fuel. When the cost of using electrical energy is four times the cost of using diesel fuel, the E-turbo is still used to increase the turbocharger rotational speed, and the E-crank is not used at all. The green $\times$-marks in top plot in Figure 6 show the consumed fuel mass for different β-values. When β is around 2, there is a large difference in consumed fuel mass. This is probably due to the efficiency of the electric motors being approximately twice the efficiency of the CI combustion engine, but there are other possible reasons, such as the non-stationary character of the mission. The bottom plot in Figure 6 shows that there is a noticeable difference in total energy cost of performing the acceleration when the E-turbo and E-crank is used, compared to using either one or the other.

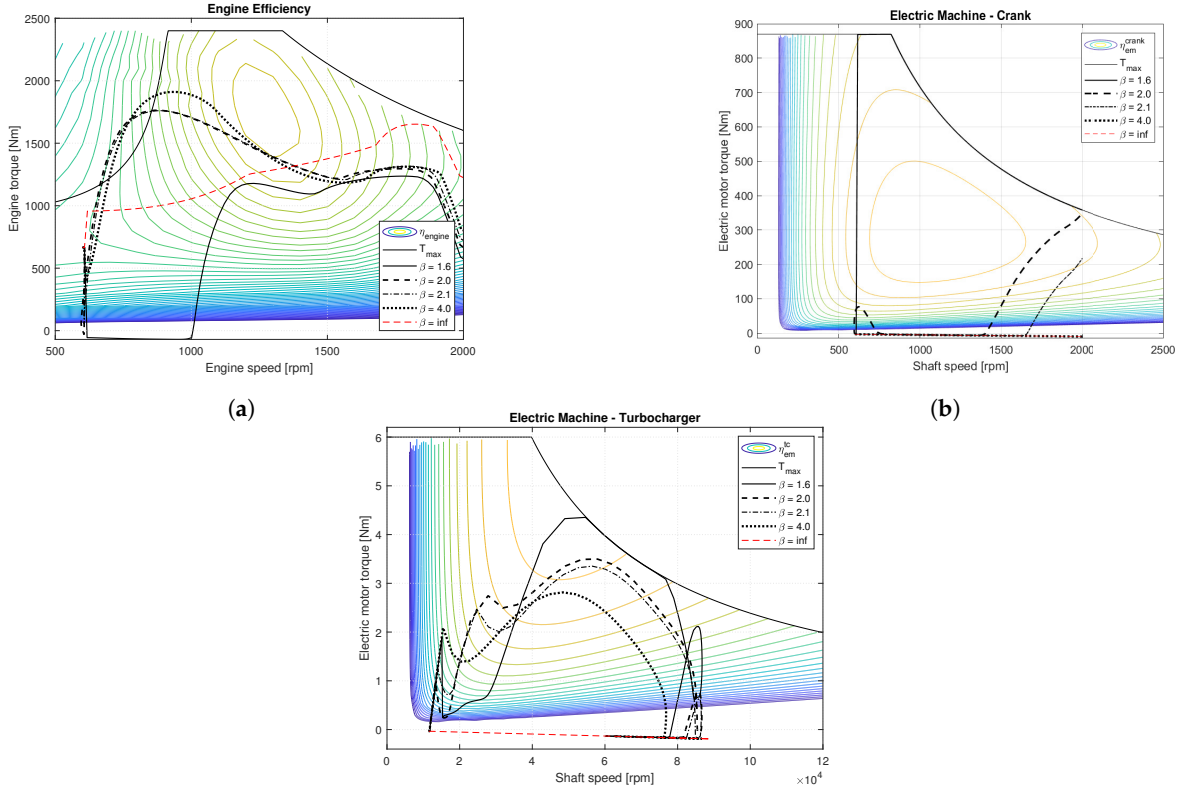

(**a**) (**b**) (**c**)

Figure 11. Solution characteristics when using a combustion engine, a crank shaft electric motor and a turbocharged electric motor. The legends display the cost factors (β) for the different solutions. (**a**) Diesel engine utilization during an optimal fuel acceleration with E-crank and E-turbo. (**b**) Utilization of the E-crank during the acceleration. When β = inf, the torque output is lower than 0 during the acceleration due to the electric motor friction. (**c**) Utilization of the E-turbo during the acceleration. When β = inf, the electric motor torque is negative due to friction.

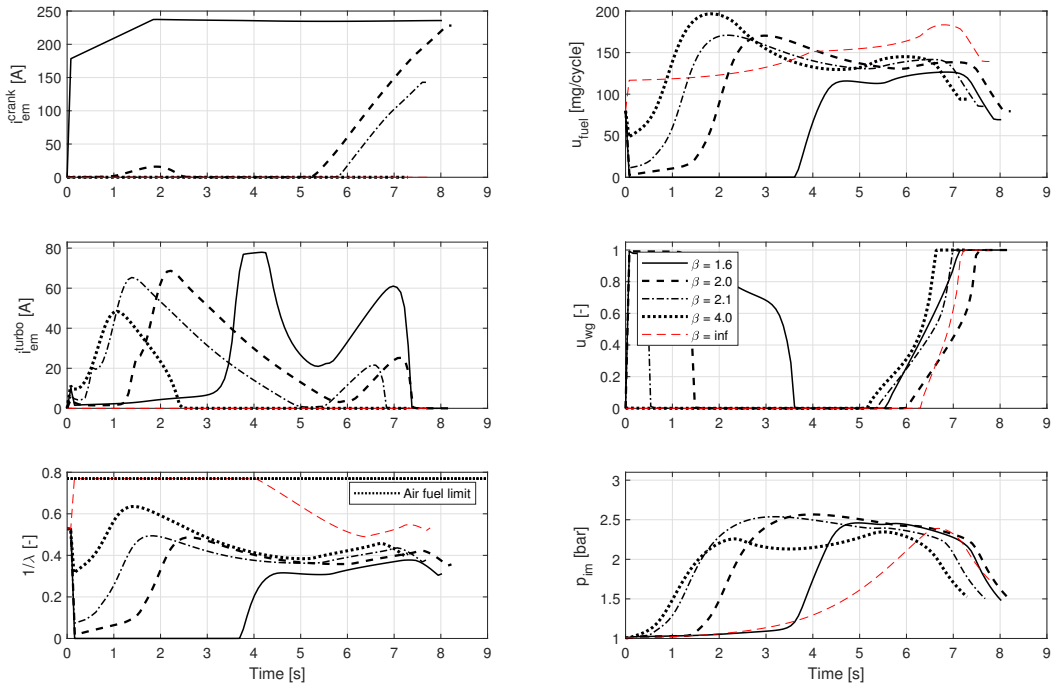

Figure 12. Controls, fuel-air ratio and intake manifold pressure during the acceleration when the engine is supported by both E-crank and E-turbo.

4.7. Analysis–Fixed Gear Acceleration

The utilization of the E-crank in Sections 4.5 and 4.6 show that the E-crank current $i_{\text{em}}^{\text{crank}}$ is reduced in the middle of the engine speed range, for the mid-range β-values. The reason is, most likely, the possibility to support the engine in the load points where the engine efficiency is relatively low. See, for example, $\beta = 2.2$ in Figure 9b, where the E-crank supports the diesel engine when the engine speed is lower than 1100 rpm and exceeds 1600 rpm. The results in Section 4.4 and Figure 8 show that the fuel injection u_{fuel} is reduced immediately at the start of the acceleration, while the E-turbo current $i_{\text{em}}^{\text{tc}}$ is increased. The strategy, when the E-turbo is used, seems to increase the boost pressure p_{im}, before the fuel is injected. One reason for this might be due to the increased boost pressure, which reduces the pumping losses in the diesel engine resulting in an increased engine efficiency. The E-turbo is also used to increase the boost pressure, before the fuel injection is increased. This can be seen in Figure 12 when $\beta = 1.6$; the truck is propelled by the E-crank the first four seconds. A short time instant before the fuel injection is increased at four seconds, the E-turbo current is increased. The result is an increased boost pressure, which reduces the time spent at the air–fuel ratio limit when the fuel injection is increased. Without the E-turbo, the response of the turbocharger would be a lot slower. The turbocharger response can be seen by comparing the β = inf solution with any of the other solutions where the E-turbo is used, by comparing the turbocharger boost pressure p_{im} in Figure 12.

5. Results—Acceleration 8–80 km/h

Acceleration using multiple gears and allowing both E-turbo and E-crank to be used during the mission was performed. The controls during the acceleration in Figure 13 show that both the E-turbo and E-crank are used during the accelerations when electrical energy is allowed. When β increases, the use of the E-crank reduces in the beginning of the acceleration. In comparison to the fixed-gear acceleration where the E-crank was used at the end of the fixed-gear acceleration ($i_{\text{em}}^{\text{crank}}$ Figure 12), the E-crank was used at the end of the complete acceleration ($i_{\text{em}}^{\text{crank}}$ Figure 13), not at the end of each gear's use. The acceleration time is similar for the different β-values, but the usage of diesel fuel is reduced with decreasing β (see Figure 13). The E-turbo current is high at the beginning of each gear's use; the amplitude of the current profile following each gear change is reduced with increasing beta. The bar plot in Figure 14 shows the energy consumption in the system, calculated as:

$$E_{\text{electric}}^{\text{turbo}} = \frac{U_{\text{terminal}}}{3600 \times 10^3} \int_{t_0}^{t_f} i_{\text{em}}^{\text{tc}}\, dt \quad [\text{kWh}] \tag{31}$$

$$E_{\text{electric}}^{\text{crank}} = \frac{U_{\text{terminal}}}{3600 \times 10^3} \int_{t_0}^{t_f} i_{\text{em}}^{\text{crank}}\, dt \quad [\text{kWh}] \tag{32}$$

$$E_{\text{fuel}} = \frac{Q_{\text{LHV}}^{\text{Diesel}}}{3600 \times 10^3} \int_{t_0}^{t_f} \dot{m}_{\text{fuel}}\, dt \quad [\text{kWh}] \tag{33}$$

The collector terms are calculated as:

$$\text{Energy input} = E_{\text{electric}}^{\text{turbo}} + E_{\text{electric}}^{\text{crank}} + E_{\text{fuel}} \quad [\text{kWh}] \tag{34}$$

$$\text{Energy output} = \frac{1}{3600 \times 10^3} \int_{t_0}^{t_f} \omega_{\text{ice}} \left(T_{\text{ice}} + T_{\text{em}}^{\text{crank}}\right) dt \quad [\text{kWh}] \tag{35}$$

$$\text{Energy saving} = \left(E_{\text{electric}}^{\text{turbo}} + E_{\text{electric}}^{\text{crank}} + E_{\text{fuel}}\right)_{\beta} - \left(\underbrace{E_{\text{electric}}^{\text{turbo}}}_{=0} + \underbrace{E_{\text{electric}}^{\text{crank}}}_{=0} + E_{\text{fuel}}\right)_{\beta=\text{inf}} \quad [\text{kWh}] \tag{36}$$

$$\text{Fuel saving} = (E_{\text{fuel}})_{\beta} - (E_{\text{fuel}})_{\beta=\text{inf}} \quad [\text{kWh}] \tag{37}$$

The bar plot in Figure 14 show that the total energy input to the system decrease as β decrease. When β increase, the energy saving decrease. The fuel cost reduction show similar behavior. When β = 2.5, more energy is spent in the E-turbo than on the E-crank.

The amount of saved energy is larger than the change in energy input to the system, when comparing the results with the fuel only solution. The reason is the E-turbo's ability to allow a higher torque output from the diesel engine in load points where the exhaust gas energy is too low to keep the intake manifold pressure high. For the three β values 1.9, 2.0 and 2.5, the amplification from spent electrical energy, to total energy savings in relation to the fuel only case are 1.53, 1.81 and 4.57. The interpretation of the amplification factor is: If 1 kWh of electric energy is consumed by the two electric motors, savings of 1.53–4.57 kWh of total energy required into the system to perform the acceleration are achieved, depending on the assigned beta value. For the same three β-values, the possible diesel fuel savings during the acceleration are 28% to 8% when beta ranges from 1.9 to 2.5. The highest amplification factor value is achieved when a major part of the energy input is used to power the electric turbocharger.

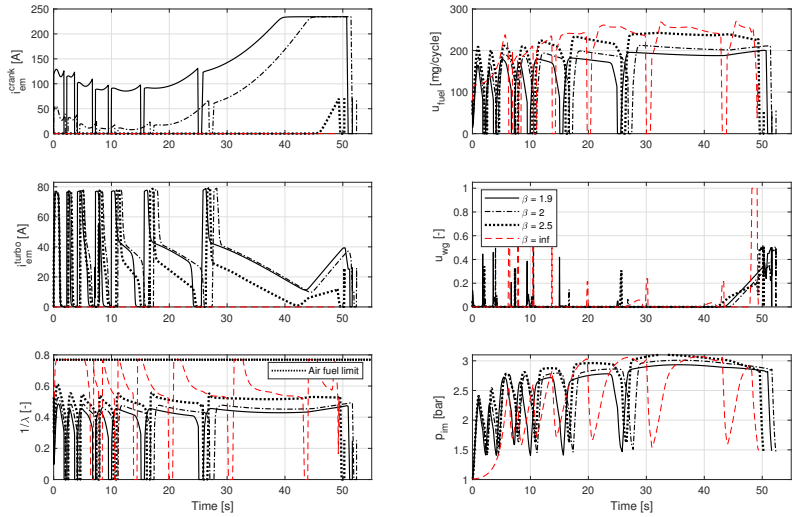

Figure 13. Controls, fuel-air ratio and intake manifold pressure during the acceleration from 8 to 80 km/h when both E-crank and E-turbo are used.

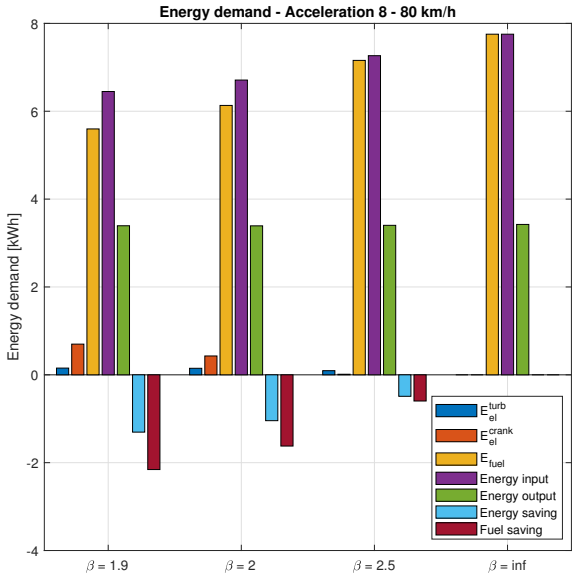

Figure 14. Consumed energy for different values of β during an acceleration from 8 to 80 km/h. The "Energy input" bar is the sum of the electrical energy and the diesel fuel. The "Energy output" bar is the work delivered to the engine main shaft. "Fuel saving" and "Energy saving" bars are relative to the minimum fuel solution (β = inf).

5.1. Analysis—Acceleration 8–80 km/h

Comparing the results when solving a fixed-gear acceleration with the full acceleration, show that the E-crank behavior is not repeated for each gear when solving the full acceleration. The reason for using the E-crank at the end of the acceleration is probably due to the added torque from the electric motor not reducing the diesel engine efficiency as much, as if it would be added when the vehicle speed is lower which results in a lower engine load. The fact that the strategy changes when the fixed-gear acceleration is changed to a full acceleration suggests that the specific acceleration of interest should be investigated, not each gear individually. Comparing the E-turbo utilization between the fixed-gear, and full acceleration, shows that the E-turbo current is high at the beginning of each gear change. p_{im} in Figure 13 shows that the extra input of electric energy to the E-turbo right after the gear change results in a rapid increase of the turbocharger boost pressure when the new gear is engaged. The E-turbo current peak is not as noticeable in the fixed-gear solution, as in the results from the full acceleration. From a system perspective, the choice of β can be made either to have a high amplification from spent electrical energy in relation to the total energy savings achieved, or to use the electrical energy for propulsion and thereby save diesel fuel. In other words, the selection has effect on the fuel saving potential in relation to the spent electrical energy budget. The decision about if the acceleration should be performed with low or high support from the electrical motors can be made if also taking the electrical energy production source into account. If the electrical energy is produced at, for example, a coal plant, a high amplification factor for the spent electrical energy can be selected to ensure that each spent Joule of electrical energy has high impact on the reduced energy need to perform the acceleration. If the stored electrical energy is produced from a green energy source, then it should be more beneficial from an environmental perspective, to use as much electrical energy as possible during the acceleration, to reduce the use of diesel fuel.

5.2. Deployment

The interpretation of the electrical energy cost factor β is to be used in a supervisory controller. The cost factor could be used in a supervisory control, which determines the power split between diesel engine and the two electric motors.

6. Conclusions

The conclusions from the two energy-optimal acceleration scenarios show how the controls of the electric motors should be defined. Different costs of electrical energy in relation diesel were compared, where larger β values represent higher costs for electrical energy.

The conclusions from our studying fuel-optimal acceleration from 600 to 2000 rpm using a fixed-gear are:

- The E-turbo is used to increase the boost pressure, which effectively enables higher torque in the beginning of the acceleration.
- When the electricity is cheap, both motors are used. When β exceeds 2.5, the E-crank is not used for propulsion, but the E-turbo still supports the diesel engine.
- The E-crank motor reduces the load from the combustion engine when $\beta < 2.5$. When β is only slightly smaller than 2.5, the E-crank is used at the end of the gear. The usage of the E-crank increases with decreasing cost factor β. Decreasing β results in a gradually increasing electric motor power, while the injected amount of fuel is decreased.
- The E-turbo is used at the beginning of the acceleration for a large range of β-values; the reason is that the smoke limit is effectively handled with the increased boost pressure. A small β-value results in the E-turbo running on full power during almost the full acceleration. A larger β-value results in the E-turbo being used at the beginning of the acceleration instead.

The full acceleration from 8 to 80 km/h results in the following conclusions:

- Using the E-crank and E-turbo reduces the total energy cost to perform the acceleration.
- The E-crank motor is used at the end of the acceleration when β is large.
- The E-turbo runs on high power in the beginning of each gear. The high power output is larger when running the full acceleration, compared to the fixed-gear scenario.

Author Contributions: Conceptualization, K.E. and L.E.; methodology, K.E.; software, K.E.; validation, K.E. and C.S.; formal analysis, K.E.; investigation, K.E.; writing—original draft preparation, K.E.; writing—review and editing, K.E., L.E. and C.S.; visualization, K.E.; supervision, L.E. and C.S.; All authors have read and agreed to the published version of the manuscript.

Funding: This research was funded by Linköping Center for Sensor Informatics and Control (LINKSIC), grant number 2016-05152.

Institutional Review Board Statement: Not applicable.

Informed Consent Statement: Not applicable.

Data Availability Statement: Not applicable.

Acknowledgments: Scania CV AB is acknowledged for contributing with discussions during the ongoing work.

Conflicts of Interest: The authors declare no conflict of interest. The funders had no role in the design of the study; in the collection, analyses, or interpretation of data; in the writing of the manuscript, or in the decision to publish the results.

References

1. ACEA Report Vehicles in Use Europe 2017. Available online: https://www.acea.be/statistics/article/vehicles-in-use-europe-2017 (accessed on 14 July 2020).
2. Medium and Heavy Trucks over 3.5 T New Registrations by Fuel Type in the European Union. Available online: https://www.acea.be/uploads/press_releases_files/ACEA_trucks_by_fuel_type_full-year_2019.pdf (accessed on 14 July 2020).
3. Hannan, M.; Azidin, F.; Mohamed, A. Hybrid electric vehicles and their challenges: A review. *Renew. Sustain. Energy Rev.* **2014**, *29*, 135–150. [CrossRef]
4. Cheng, C.; McGordon, A.; Jones, R.P.; Jennings, P.A. Generalised fuzzy-logic-based power management strategy for various hybrid electric vehicle powertrain architectures. In Proceedings of the UKACC International Conference on Control 2010, Coventry, UK, 7–10 September 2010; pp. 1–6.
5. Uebel, S.; Murgovski, N.; Tempelhahn, C.; Bäker, B. Optimal Energy Management and Velocity Control of Hybrid Electric Vehicles. *IEEE Trans. Veh. Technol.* **2018**, *67*, 327–337. [CrossRef]
6. Johannesson, L.; Murgovski, N.; Jonasson, E.; Hellgren, J.; Egardt, B. Predictive energy management of hybrid long-haul trucks. *Control. Eng. Pract.* **2015**, *41*, 83–97. [CrossRef]
7. Karbowski, D.; Delorme, A.; Rousseau, A. *Modeling the Hybridization of a Class 8 Line-Haul Truck*; SAE 2010 Commercial Vehicle Engineering Congress; SAE International: Warrendale, PA, USA, 2010; [CrossRef]
8. Wang, R.; Lukic, S.M. Dynamic programming technique in hybrid electric vehicle optimization. In Proceedings of the 2012 IEEE International Electric Vehicle Conference, Greenville, SC, USA, 4–8 March 2012; pp. 1–8; [CrossRef]
9. Dib, W.; Serrao, L.; Sciarretta, A. Optimal control to minimize trip time and energy consumption in electric vehicles. In Proceedings of the 2011 IEEE Vehicle Power and Propulsion Conference, Chicago, IL, USA, 6–9 September 2011; pp. 1–8; [CrossRef]
10. Murgovski, N.; Johannesson, L.; Sjöberg, J.; Egardt, B. Component sizing of a plug-in hybrid electric powertrain via convex optimization. *Mechatronics* **2012**, *22*, 106–120. [CrossRef]
11. Xiao, B.; Hellström, E.; Kelly, T.; Stolzenfeld, T.; Bell, D.; Jankovic, M.; Buckland, J.H.; Rollinger, J. Dynamic Pressure Ratio Allocation for Electric Supercharger and Turbocharger Coordination. In Proceedings of the 2018 Annual American Control Conference (ACC), Milwaukee, WI, USA, 27–29 June 2018; pp. 2455–2460.
12. Millo, F.; Mallamo, F.; Pautasso, E.; Ganio Mego, G. *The Potential of Electric Exhaust Gas Turbocharging for HD Diesel Engines*; SAE 2006 World Congress & Exhibition; SAE International: Warrendale, PA, USA, 2006; [CrossRef]
13. Kolmanovsky, I.; Stefanopoulou, A.G. *Evaluation of Turbocharger Power Assist System Using Optimal Control Techniques*; SAE 2000 World Congress; SAE International: Warrendale, PA, USA, 2000. [CrossRef]
14. Hopmann, U.; Algrain, M.C. *Diesel Engine Electric Turbo Compound Technology*; SAE Technical Paper; SAE International: Warrendale, PA, USA, 2003. [CrossRef]
15. Nezhadali, V.; Sivertsson, M.; Eriksson, L. Turbocharger Dynamics Influence on Optimal Control of Diesel Engine Powered Systems. *SAE Int. J. Eng.* **2014**, *7*, 6–13. [CrossRef]

16. Jain, A.; Nuesch, T.; Nagele, C.; Lassus, P.; Onder, C. Modeling and Control of a Hybrid Electric Vehicle With an Electrically Assisted Turbocharger. *IEEE Trans. Veh. Technol.* **2016**, *65*, 1. [CrossRef]
17. Guzzella, L.; Sciretta, A. *Vehicle Propulsion Systems*; Springer: Berlin/Heidelberg, Germany, 2007.
18. Ekberg, K.; Leek, V.; Eriksson, L. Modeling and Validation of an Open-Source Mean Value Heavy-Duty Diesel Engine Model. *Simul. Notes Eur.* **2018**, *28*, 197–204. [CrossRef]
19. Heywood, J.B. *Internal Combustion Engine Fundamentals*, 2nd ed.; McGraw-Hill Education: New York, NY, USA, 2018.
20. Galindo, J.; Serrano, J.; Guardiola, C.; Cervelló, C. Surge limit definition in a specific test bench for the characterization of automotive turbochargers. *Exp. Therm. Fluid Sci.* **2006**, *30*, 449–462. [CrossRef]
21. Sundström, C.; Frisk, E.; Nielsen, L. A new electric machine model and its relevance for vehicle level diagnosis. *Int. J. Model. Identif. Control* **2015**, 24, 1–19. [CrossRef]
22. Ibaraki, S.; Yamashita, Y.; Sumida, K.; Ogita, H.; Jinnai, Y. *Development of the "Hybrid Turbo", an Electrically Assisted Turbocharger*; Technical Review; Mitsubishi Heavy Industries, Ltd.: Tokyo, Japan, 2006; Volume 43.
23. The MathWorks, Inc. *Statistics and Machine Learning Toolbox Release*; The MathWorks, Inc.: Natick, MA, USA, 2019.
24. Eriksson, L.; Larsson, A.; Thomasson, A. The AAC2016 Benchmark—Look-Ahead Control of Heavy Duty Trucks on Open Roads. *IFAC* **2016**, *49*, 121–127. [CrossRef]
25. Wong, J.Y. *Theory of Ground Vehicles*; John Wiley & Sons, Inc.: Hoboken, NJ, USA, 2008.
26. Leek, V. An Optimal Control Toolbox for MATLAB Based on CasADi. Master's Thesis, Linköping University, Vehicular Systems, Linköping, Sweden, 2016.
27. Andersson, J.A.E.; Gillis, J.; Horn, G.; Rawlings, J.B.; Diehl, M. CasADi—A software framework for nonlinear optimization and optimal control. *Math. Program. Comput.* **2019**, *11*, 1–36. [CrossRef]
28. Wächter, A.; Biegler, L. On the implementation of a primal-dual interior point filter line search algorithm for large-scale nonlinear programming. *Math. Program.* **2006**, *106*, 25–57. [CrossRef]
29. Ekberg, K.; Eriksson, L. *Development and Analysis of Optimal Control Strategy for Gear Changing Patterns During Acceleration*; IFAC Papersonline; Elsevier: Amsterdam, The Netherlands, 2019; Volume 52, pp. 316–321. [CrossRef]
30. Ekberg, K.; Eriksson, L. *A Comparison of Optimal Gear Shifts for Stiff and Flexible Driveshafts During Accelerations*; IFAC World Congress 2020; Viritual: Berlin, Germany, 2020.